Adsorption 2, 205–216 (1996)

Application of the Thermal Frequency Response Method and of Pulsed Field Gradient NMR to Study Water Diffusion in Zeolite NaX

VINCENT BOURDIN
LIMSI-CNRS, BP 133, F91403 Orsay, France

ANDREAS GERMANUS
Universität Leipzig, Fakultät für Physik und Geowissenschaften, Linnéstr. 5, D-04103 Leipzig, Germany; and Bruker-Franzen Analytik GmbH, Fahrenheitstr. 4, D-28359 Bremen, Germany

PHILIPPE GRENIER
LIMSI-CNRS, BP 133, F91403 Orsay, France

JÖRG KÄRGER
Universität Leipzig, Fakultät für Physik und Geowissenschaften, Linnéstr. 5, D-04103 Leipzig, Germany

Received July 17, 1995; Revised December 14, 1995; Accepted December 27, 1995

Abstract. The thermal frequency response and pulsed field gradient NMR methods are applied in a comparative study of water diffusion in zeolite NaX under non-equilibrium and equilibrium conditions. The obtained results are found to be in satisfactory agreement with each other, indicating that by applying the thermal frequency response method, complications due to uncontrolled water adsorption at the chamber walls inherent in conventional frequency response measurements may be circumvented.

Keywords: diffusion, kinetic measurements, NaX zeolite, water

Introduction

In many cases, intracrystalline molecular propagation is one of the controlling mechanisms in zeolite mass transfer. Moreover, zeolitic adsorbent-adsorbate systems are considered to be an ideal model system for the study of molecules in contact with solid surfaces, in particular for the study of their dynamic behaviour. Numerous investigations have been carried out to study molecular diffusion in zeolites (Weisz, 1975; Ruthven, 1984; Barrer, 1978; Kärger and Ruthven, 1992; Chen et al., 1994; Bülow and Micke, 1995). Researchers in the field of zeolitic diffusion were particularly intrigued by the fact that occasionally the information about intracrystalline mobility, as deduced from microscopic equilibrium measurements, was in conflict with the data obtained in macroscopic non-equilibrium experiments. There are examples where the diffusivities obtained by these two different methods are in good agreement (e.g., *n*-paraffins, xenon and carbon dioxide in NaCaA (Heink et al., 1992; Ruthven, 1993), ethane in ZSM-5 (Van den Begin and Rees, 1989) and methanol in NaX (Grenier et al., 1994)), while in other cases substantial differences were observed (e.g. *n*-paraffins in NaX (Ruthven et al., 1991). The clarification of the origin of this discrepancy is a current topic of zeolite research (Kärger and Ruthven, 1992; Garcia and Weisz, 1990; Rees, 1994), and there is a great need for accurate diffusion data for a large spectrum of well-defined adsorbent-adsorbate systems,

obtained by both equilibrium and non-equilibrium methods.

It is interesting to note that with the exception of the very first systematic studies of zeolitic diffusion (Tiselius, 1934; Barrer and Fender, 1961), water has not been the subject of comparative diffusion experiments either under equilibrium or non-equilibrium conditions. This is rather surprising since, in view of the particular role of water in nature, water diffusion studies are of substantial relevance for both fundamental research and practical applications. This lack of experimental evidence is most likely due to difficulties which are encountered when studying water diffusion in zeolites. Firstly, it cannot be excluded that under the influence of consecutive cycles of water adsorption and thermal reactivation there may be a partial damage of the crystalline structure which eventually affects the intracrystalline diffusivities. Secondly, non-equilibrium measurements with water are complicated by the possibility of water adsorption on the walls of the adsorption vessel.

In the present study we have tried to reduce possible complications due to these two reasons. We have employed the recently proposed thermal frequency response method (Bourdin et al., 1996) as a non-equilibrium technique. Correlating the responses of the pressure and temperature to a peroidic change of the volume of the adsorption vessel, this technique proved not to be affected by water adsorption on the walls. Moreover, by using the thermal frequency response method it is much easier to decide whether the observed adsorption/desorption behaviour is controlled by thermal relaxation or by transport effects (i.e., diffusion or permeation through surfaces). Since the rate of molecular adsorption/desorption may be affected by any of these processes in roughly the same way, uptake retardation by the finite rate of adsorption heat release may be misinterpreted as an effect of the reduced mobility (Kärger and Ruthven, 1992). In fact, in many cases the finite rate of heat release seems to provide the explanation for the discrepancy between the previous non-equilibrium and equilibrium diffusion measurements. Direct measurement of the sample temperature in the thermal frequency response method provides the means of analyzing the influence of heat and transport effects on the adsorption/desorption rates. The fundamentals of this technique are described in Bourdin et al. (to be published) and summarized in the following section.

Pulsed field gradient (PFG) NMR method has proved to be a rather sensitive tool for studying structure-related transport properties of adsorbent-adsorbate systems (Kärger and Ruthven, 1992). We applied this technique in order to estimate the range and the trends of the water diffusivities in zeolite NaX using samples obtained from different batches and under different pretreatments conditions. The thermal frequency response method gives an access to the mass transfer characteristic time, and thus requires the use of zeolite crystallites with diameters as large as possible when fast mass transfer kinetics is involved. Only a limited quantity of the large crystals (100 μm) was available in this study, a quantity which was not sufficient for the use of PFG NMR measurements.

Fundamentals of the Thermal Frequency Response Method

The thermal frequency response (TFR) method is a modification of the conventional frequency response method (Rees, 1994; Yasuda, 1994). In this method an adsorbent sample is placed in a chamber whose volume V varies periodically at an angular frequency ω:

$$V = V_e(1 - ve^{i\omega t}) \tag{1}$$

The subscript e indicates the mean value of the given parameter. The modulation amplitude of the volume, v, is kept constant when varying ω. After a transient period, the pressure becomes a periodical function of the time at the same frequency. We may write therefore:

$$P = P_e[1 + pe^{i(\omega t+\psi)}] \tag{2}$$

or

$$\Delta P/\Delta V = \frac{p}{v}e^{i\psi} \tag{3}$$

where $\Delta V = (V_e - V)/V_e$ and $\Delta P = (P - P_e)/P_e$ are respectively the relative volume and pressure variations around their mean values. The ratio $\Delta P/\Delta V$ is independent of time and the response is quasi-stationary. The relative amplitude p and the phase ψ of the pressure response are functions of the frequency ω and are determined by the thermodynamic and kinetic properties of the sample. In general, the experimental results are represented in terms of the so-called in-phase and out-of-phase functions δ_{in} and δ_{out} defined by the following relation:

$$\Delta V/\Delta P - 1 = \delta_{in} - i\delta_{out} \tag{4}$$

In the TFR method both temperature and pressure are measured. The change of the pressure due to the volume change induces a change of the adsorbed amount. The heat of sorption released or consumed during this process leads to a change of the sample temperature which is measured by infrared detection. Like pressure, temperature is also a periodic function of time:

$$T = T_e + A_T e^{i(\omega t+\varphi)} \tag{5}$$

which may also be written as:

$$\Delta T/\Delta V = \frac{A_T}{v} e^{i\varphi} \tag{6}$$

with $\Delta T = T - T_e$ denoting the temperature variation around the constant temperature of the wall. The in-phase and out-of-phase functions θ_{in}^v and θ_{out}^v of the TFR method (Bourdin et al., 1996) are defined as the real and imaginary parts of this complex ratio multiplied by the volume amplitude v:

$$\theta_{\text{in}}^v + i\theta_{\text{out}}^v = v\Delta T/\Delta V \tag{7}$$

This ratio is again independent of time, and the amplitude A_T and phase φ of the temperature response are functions of the frequency.

The variation of the sample temperature is due to the thermal effects associated with the change of the adsorbed amount as a consequence of the pressure change. Ideally, the pressure variation as induced by the volume variation is only a function of the adsorption properties of the sample. In reality, however, the pressure change may be influenced by additional factors like adsorption by the chamber walls and temperature effects by non-isothermal compression. It is often advisable, therefore, to express the temperature as a function of the pressure. By combining Eqs. (3) and (6) one obtain:

$$v\Delta T/\Delta P = \theta_{\text{in}}^p + i\theta_{\text{out}}^p = \frac{v}{p} A_T e^{i(\varphi-\psi)} \tag{8}$$

The characteristic functions θ_{in}^p and θ_{out}^p may be directly obtained from the experimental temperature data, taking the experimental pressure data as a reference. They are very useful since they describe the intrinsic behavior of the sample, independently of all side effects.

The sample considered thereafter is assumed to consist of crystals of uniform size subjected to the same physical conditions. For the calculation of the time dependence of the temperature and pressure variation we use a non-isothermal model described elsewhere (Sun et al., 1993). It assumes that the mass transfer is subjected to Fickian diffusion in the intracrystalline bulk phase and/or to surface barriers at the gas-crystal interface. The equations of heat and mass transfer may be written as follows.

Overall mass balance:

$$\frac{d}{dt}\left(\frac{PV}{RT} + V_s\bar{q}\right) = 0 \tag{9}$$

where V_s is the sample volume, $\bar{q}$ is the average concentration of the sorbate and R is the gas constant.

Mass balance in the crystal, with accompanying boundary and initial conditions:

$$\begin{aligned} \frac{\partial q}{\partial t} &= \frac{D_T}{r_c^\sigma}\frac{\partial}{\partial r_c}\left(r_c^\sigma \frac{\partial q}{\partial r_c}\right); \\ -D_T \left.\frac{\partial q}{\partial r_c}\right|_{r_c=R_c} &= k(q|_{r_c=R_c} - q^*); \\ \left.\frac{\partial q}{\partial r_c}\right|_{r_c=0} &= 0 \end{aligned} \tag{10}$$

where σ is a shape factor ($\sigma = 0$, 1 or 2 for sheet, cylinder or sphere, respectively), D_T is the intracrystalline diffusion coefficient, k is the surface barrier coefficient and R_c is the crystal radius. Since the amplitude of the volume change is small (~0.02), the adsorption isotherm may be linearized and the amount adsorbed at equilibrium (q^*) is given by:

$$q^* - q_e = K_p(P - P_e) - K_T(T - T_e) \tag{11}$$

where q_e is the concentration at thermodynamic equilibrium for $P = P_e$ and $T = T_e$. Energy balance in the crystal:

$$C_s\frac{dT}{dt} + \frac{(\sigma+1)h}{R_c}(T - T_e) = |\Delta H|\frac{d\bar{q}}{dt} \tag{12}$$

where C_s is the volumetric heat capacity of the crystals, h the heat transfer coefficient and ΔH the enthalpy of sorption.

In our investigation, the temperature is considered to be uniform across the crystals. This assumption may be justified by an order-of-magnitude estimate of the characteristic time of heat dissipation within the crystal. With reasonable assumptions for the overall heat

capacity ($C_s \sim 2 \times 10^6$ Jm^{-3}K^{-1}) and the heat conductivity ($\lambda > 0.4$ Wm^{-1}K^{-1}) of the zeolite crystallites (Sahnoune and Grenier, 1989) one obtains a value of less than 1 ms, which is the smallest characteristic response time in our experiment.

For visualising the fundamentals of the TFR method, we will first consider the evolution of the temperature and pressure after a single step. Starting from equilibrium at pressure P_0 and temperature T_0 the bellows is suddenly compressed at time $t = 0$. The pressure rises instantaneously to its maximum value P_M and decreases monotonically towards the final pressure P_f due to the adsorption in the sample. The adsorption occurs at first under the concentration gradient caused by the pressure change and then by the temperature decrease due to the dissipation of the heat of adsorption ("thermal relaxation"). The temperature behaviour is different: at first the temperature rises due to the heat released by the adsorption. After passing a maximum, the temperature again decreases and approaches its initial value T_0. Figure 1 shows a typical time dependency of the pressure and the temperature after a single step.

We will now consider that the bellows is decompressed after a time interval $\Theta/2 = \pi/\omega$ and compressed again at time Θ, and so on, i.e., the volume is assumed to change by square waves with periodicity Θ. The overall response may be constructed by adding the response while the bellows is compressed and by subtracting the response while it is expanded. After a transient time the response is quasi-stationary and has the same absolute value during the last half period as during the first one, but with opposite signs. Thus it is sufficient to analyse the response during the first half period.

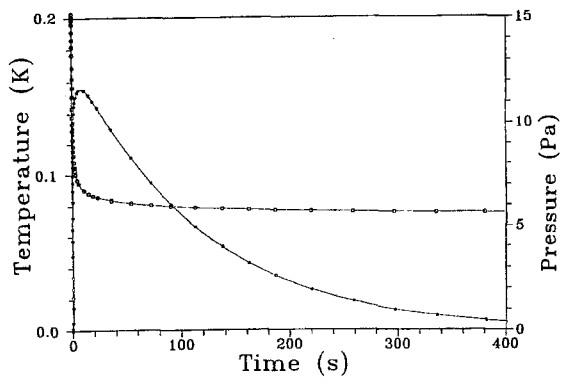

Figure 1. Typical volume step response. (∗ ∗ ∗) temperature and (o o o) pressure. The data are taken from an experiment on NaX 1 mm pellets (2 μm crystals binded with a clay) with water.

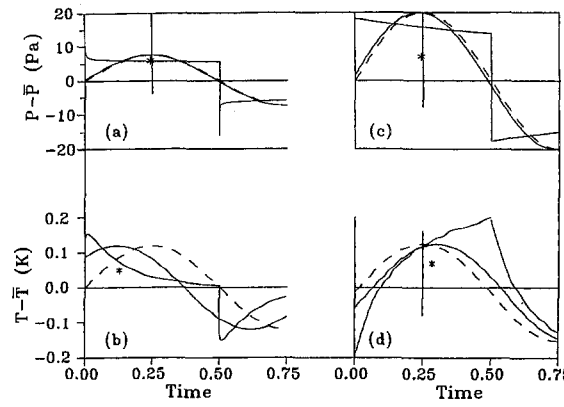

Figure 2. Square wave half period response of pressure (top) and temperature (bottom) in the low frequency (left, period 800 s) and high frequency (right, period 0.32 s) modes. (∗) is the mean coordinates point averaged over the half period. (____) Fundamental harmonic of the pressure or temperature response and (− − −) fundamental harmonic of the square wave volume variation.

Let us first consider the case of low frequencies, i.e., we suppose that Θ is very large compared with the overall characteristic time of the sample response. In this case, over almost the total first half period $0 - \Theta/2$ the pressure is equal to P_f as shown in Fig. 2a. Consequently, the mean value Y of the pressure response during this interval is close to P_f and the mean value X of the time weighted by the pressure amplitude is in the middle of the interval. In the figure, the point G (coordinates X, Y) is marked by an asterisk. Its position relative to the middle of the interval indicates roughly the phase shift between the pressure and the volume (with opposite sign). It turns out that the phase shift of the pressure change is close to zero.

For the temperature change the reasoning must be different because the mean amplitude is close to 0, and the signal is concentrated at the beginning. That means that, at very low frequencies, the amplitude of the temperature response is close to 0 and that the phase is close to $+\pi/2$, i.e., the temperature response is in advance with respect to the volume (Fig. 2b). As the frequency increases a thermal response appears and in case of equilibrium adsorption, its amplitude tends toward a limit A_M which is the change of the sample temperature when the chamber volume is subjected to an adiabatic compression of amplitude v. In such conditions, the phase decreases and tends towards 0. That means that the in-phase and the out-of-phase functions are positive. The out-of-phase function passes through a maximum at a frequency depending on the thermal relaxation time.

Let us now suppose that the time Θ is reduced to a value which is smaller than the characteristic time of mass transfer within the sample. $\Theta/2$ is therefore smaller than the time at which the maximum temperature occurs. The pressure response for such a case is presented by Fig. 2c. One can see that the mean value of the pressure is close to P_M. That means that the amplitude of the pressure variation is greater than the amplitude at low frequency. Moreover, the pressure is greater at the beginning than at the end of the half period: thus the phase is still positive. On the contrary, the temperature response is minimum at the beginning and increases during the half period as shown in Fig. 2d. The phase is therefore negative as indicated by the position of G. With increasing frequency the amplitude will decrease and tends towards zero. That means that the out-of-phase function is negative and passes through a minimum depending on the mass transfer characteristic time.

Let us now consider a sinusoidal volume variation instead of a square wave one. In fact, the sinusoidal volume variation may be considered as the fundamental harmonic of the square wave volume variation. Figure 2 also contains the fundamental harmonic of the pressure or temperature responses (full lines) and the fundamental harmonic of the square wave volume modulation (dashed lines). The preceding conclusions clearly remain valid for the fundamental harmonics, i.e., the phase of the pressure is always positive and the phase of the temperature is positive at low frequencies and negative at high frequencies. Figure 3 shows an actual plot of the volume, pressure and temperature changes during a typical thermal frequency response experiment: the temperature phase lag is clearly visible. The pressure phase lag is much smaller and becomes apparent only by numerical treatment.

As pointed out previously, an extremum of the out-of-phase function of the temperature response appearing at an angular frequency ω corresponds to a characteristic time t which is related to the frequency ω, at which this extremum is observed ($\omega t \sim 1$). The characteristic time corresponding to the maximum depends on the heat transfer coefficient h, while the characteristic time corresponding to the minimum depends on the mass transfer kinetic parameters D_T and/or k. Thus, each kinetic parameter corresponds to a window in the frequency domain in which this parameter affects the shape of the characteristic functions, and this influence is different depending on the nature of the parameter. A thermal effect always corresponds to an increase of the response amplitude and a mass transfer resistance corresponds to a decrease of the response amplitude when the frequency increases. Moreover, the shape of the in-phase and out-of-phase functions is different in case of Fickian diffusion and in case of surface barrier resistance as shown in Fig. 4. Thus it is quite easy to identify these parameters separately.

The characteristic times which affect the in-phase and out-of-phase functions depend on the ratio of the adsorbed mass variation over the gas mass variation in the chamber for a given variation of the pressure. This ratio (the "adsorptive capacity coefficient" K) is given by the relation:

$$K = \frac{V_s}{V_e} K_p R T_e \tag{13}$$

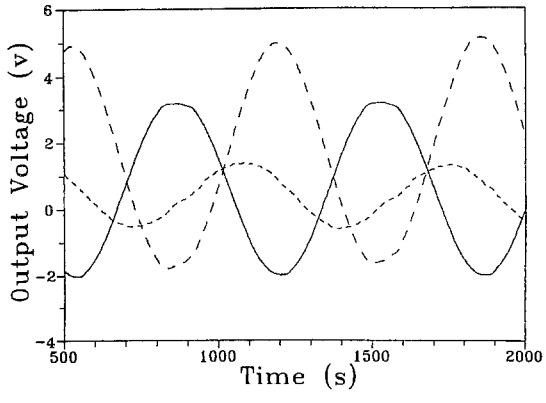

Figure 3. Recorded data during Experiment No. 3. (——) Volume. (— —) pressure. (— — —) temperature. The phase lag between volume and temperature responses is clearly visible.

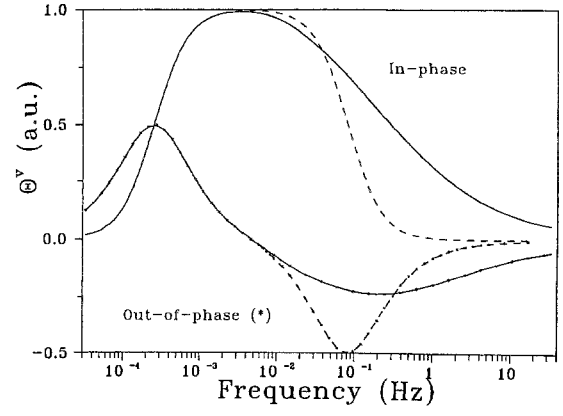

Figure 4. Characteristic temperature functions for $\tau_h = 1000$ s: (____) pure Fickian diffusion with $\tau_{Dc} = 10$ s, (— — —) pure surface barrier with $\tau_{kc} = 10$ s.

where R is the gas constant. The larger the adsorptive capacity, the faster the kinetics.

For spherical crystals, the most useful characteristic times to describe the shape of the characteristic functions are:

$$\tau_h = \frac{(1+K+\gamma)}{(1+K)}\frac{R_c C_s}{3h} \qquad \tau_D = \frac{1}{(1+K)}\frac{R_c^2}{15 D_T}$$
$$\tau_s = \frac{1}{(1+K)}\frac{R_c}{3k} \tag{14}$$

where $\gamma = |\Delta H| K_T / C_s$ is the non-isothermality coefficient. In the case where mass transfer resistances are negligible, the maximum of the out-of-phase function occurs at a frequency ω given by the relation $\omega\tau_h = 1$. Similarly, in the adiabatic case ($\tau_h = \infty$) where only surface barrier resistance exists, the frequency ω at which the minimum of the out-of-phase function occurs is given by the relation $\omega\tau_s = 1$. In the adiabatic case where the mass transfer is a pure Fickian diffusion, the relation between the frequency of the minimum of the out-of-phase function and the characteristic time τ_D is not so simple and is approximately given by the relation $\omega\tau_D \sim 0.8 + 0.3\,(K+\gamma)$.

Experimental

We used zeolite specimens of type NaX with Si/Al ratio of about 1.2 with mean crystallite diameters of 30 μm, 45 μm and 100 μm, which were synthesized by S.P. Zhdanov and co-workers in St. Petersburg, Russia, according to the procedure described in Zhdanov et al. (1981).

The PFG NMR self-diffusion experiments were carried out with loose beds of zeolite crystallites (about 300 mg) contained in NMR glass tubes with an outer diameter of 8 mm. We have applied different modes of zeolite activation, which differed from each other in the conditions of dehydration during the heating procedure as summarized in Table 1. Obviously, during activation mode 1, the "self steaming" intensity during the activation procedure is smallest, while mode 5 effects an intense hydrothermal treatment of the sample. In any of these procedures, the sample was kept for about 10 hours at the final temperature of 400°C under continuous evacuation. The final pressure was less than 10^{-2} Pa. After cooling to room temperature under continued evacuation, a well-defined amount of water molecules was introduced into the sample by adsorbing at low temperature the water vapour contained in a calibrated volume at known pressure. Afterwards the sample was sealed.

Table 1. Different modes of sample activation used for the preparation of the PFG NMR samples. The activation of the thermal FR sample corresponds to mode 2.

Mode of activation	Heating rate	Bed height	Condition of water vapour release
1	~10 K/h	<1 mm	Continuous evacuation
2	~100 K/h	<1 mm	Continuous evacuation
3	~10 K/h	~20 mm	Continuous evacuation
4	~100 K/h	~20 mm	Open vessel in contact with air
5	~100 K/h	~20 mm	Closed vessel, vapour release through a small orifice

The conditions for the application of PFG NMR worsen with decreasing transverse nuclear magnetic relaxation times (T_2). In the present system T_2 was found to decrease with decreasing concentration. As a consequence, for water concentrations below 6 molecules per cavity, PFG NMR measurements of molecular diffusion turned out to be impossible. Best measuring conditions were attained close to the saturation capacity at a sorbate concentration of about 25 molecules per cavity. The TFR and PFG NMR diffusivities were compared in these conditions.

The self-diffusion measurements were carried out on the home-built PFG NMR spectrometer FEGRIS 60 operating at a proton resonance frequency of 60 MHz (Heink et al., 1995). The coefficients of self-diffusion have been determined in the conventional way (Kärger and Ruthven, 1992) by comparing the decay of the NMR signal intensity (of the "spin echo") with increasing gradient intensity with that of a standard (water, $D = 2.04\,10^{-9}\,m^2\,s^{-1}$ at 293 K (Weingärtner, 1982)). The temperature of the sample was controlled by a stream of evaporating liquid nitrogen or preheated air.

The TFR measurements were carried out by means of the device schematically shown in Fig. 5. Details may be found in Bourdin et al. (1996). The pressure is measured by a fast Baratron gauge. The temperature is measured by infrared detection. The lower limit of the amplitude of the pressure and temperature response detectable by the device is on the order of 0.03 Pa and 0.1 mK, respectively. The smallest time constant of the pressure gauge and the infrared detector is 1 ms.

For the TFR measurements, exclusively zeolite specimens with a mean crystallite diameter of 100 μm were

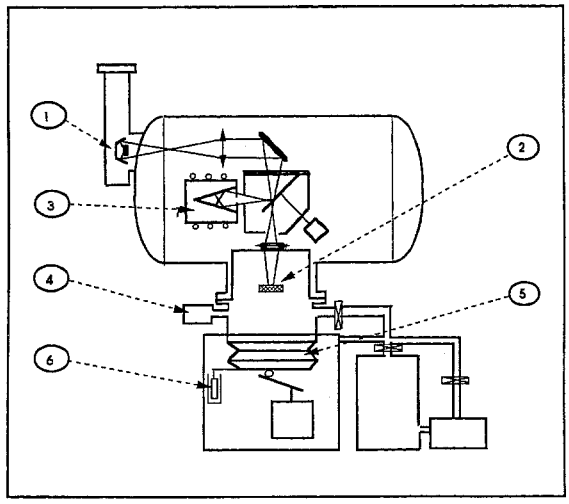

Figure 5. Experimental set up. 1: Infrared detector. 2: Sample. 3: Temperature controlled black body. 4: Pressure gauge. 5: Bellows. 6: Position gauge.

used. The experiments were performed with two different samples: a "fresh" sample of 23.5 mg with a bed height of approximately 0.15 mm subjected to a procedure corresponding to mode 2 (Sample I) and a sample which was previously used in adsorption/desorption studies with methanol (bed height ~ 0.5 mm) (Sample II). Since this sample showed some coke depositions, it had been regenerated under an atmosphere of oxygen at 380°C before it was activated in essentially the same way as Sample I. With each sample the measurements were carried out at three different temperatures: Sample I at 288 K, 297 K and 328 K (Experiments 1, 2 and 3), with the water vapours adjusted to 58 Pa, 103 Pa and 660 Pa, respectively, and Sample II at 283 K, 304 K and 343 K (Experiments 4, 5 and 6) at 37 Pa, 153 Pa and 830 Pa respectively. Figure 6 shows the adsorption isotherms of the NaX-water system as determined in this laboratory (Rios, 1984) for the temperatures of the experiments. The asterisks correspond to the experimental conditions. One can see that in all experiments the mean sorbate concentration essentially remained constant, corresponding to a loading of ~25 water molecules per cavity.

It was not possible to perform experiments at lower loadings at the ambient temperature with the present equipment, due to the loss of sensitivity of the pressure gauge (10^4 Pa full scale) and to the difficulty of maintaining the chamber at very low pressure. A new design of the chamber will permit us to reduce the working pressure to a very low value (~1 Pa).

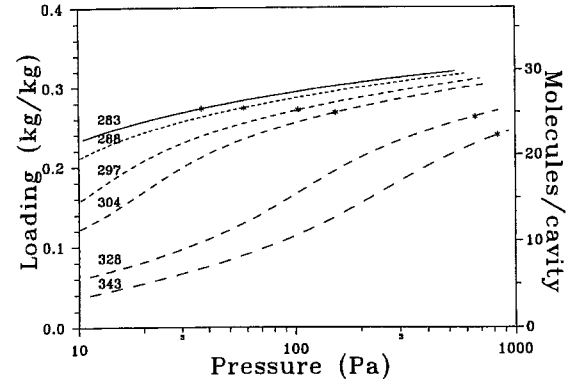

Figure 6. NaX-water isotherms for the temperatures (expressed in Kelvin) in TFR experiments. Asterisks indicate the pressure and the corresponding loading for each experiment.

Results and Discussion

PFG-NMR Results

The water diffusivities in zeolite NaX at 293 K as determined by PFG NMR for different specimens and after different modes of sample activation are plotted in Fig. 7 as a function of the sorbate concentration. In all cases, the observed mean diffusion paths were much smaller than the mean crystallites diameters, so that the obtained diffusivities represent genuine intracrystalline diffusivities. Moreover, the attenuations of the

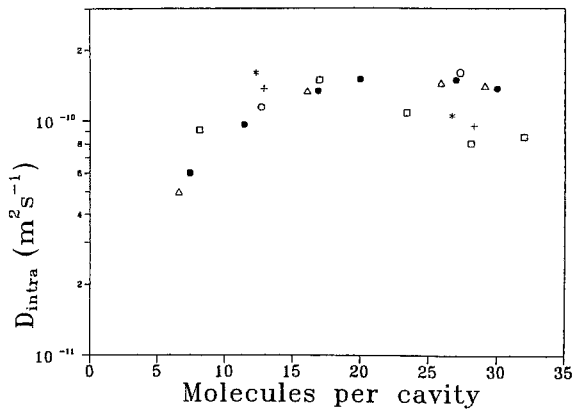

Figure 7. Concentration dependence of the diffusivity of water in zeolite NaX obtained by PFG NMR for samples stemming from different batches and for different activation procedures: (•) 45 μm crystallite diameter, activation mode 1; (○): 45 μm, mode 1 (different batch); (∗): 30 μm, mode 3, data from Kärger (1971); (+): 30 μm, material used in Kärger (1971), reactivated, mode 1; (Δ): 45 μm, mode 4; (□): 45 μm, mode 5.

NMR signal were found to be monoexponential so that there is in fact only one mode of molecular transport observed in these experiments.

It is interesting to note that for the 45 μm sample even a moderate hydrothermal pretreatment (activation mode 4) leads to essentially the same diffusivities as in the case of the rather "mild" activation mode 1. For these samples an increase of the diffusivities with increasing concentration is observed. This behaviour is in agreement with previous nuclear magnetic relaxation studies (Pfeifer, 1976; Pfeifer et al., 1978), where the first water molecules have been found to be captured by the sodalite cages and by the most intense adsorption sites (mainly cations). Since PFG NMR is observing the mobility of all molecules contributing to the spin echo, any enhancement of the concentration will lead to an enhancement of the fraction of mobile molecules and hence to an increasing overall mobility. With respect to the time scale of the PFG NMR experiment (a few milliseconds), there is a fast exchange between the molecules in these different state of mobility (Pfeifer, 1976; Pfeifer et al., 1978). A distinction between the modes of mobility in the sodalite cages and in large cavities of the NaX structure is therefore impossible.

While the diffusivities remained constant for the 45 μm samples between medium concentration and saturation, a slight decrease with increasing concentration was observed for the 30 μm sample. The same behaviour was observed for the 45 μm sample, when it had been activated according to mode 5. In an additional series of experiments the intensity of the hydrothermal pretreatment was further enhanced by keeping the sample at the final temperature of 400°C over 24 hours without releasing the water vapour. In this case, a distinct deviation from a monoexponential behaviour of the NMR signal attenuation was observed indicating that this type of pretreatment had caused a partial destruction of the zeolite framework. Since Sample 3 showed a similar pattern of concentration dependence, it is most likely that also this zeolite specimen contains slight structural defects. Correspondingly, X-ray diffraction studies of this sample revealed a large contribution of amorphous material within the sample. It is remarkable that the water diffusivities measured in this very sample more than twenty years ago (Kärger, 1971) could be reproduced in the present study. This means that over such a large period of time the zeolite structure remained unchanged.

The results presented in Fig. 7 show that even after rather different modes of zeolite activation as well as for zeolite specimens from different batches, the scattering in the NMR diffusivities remains within a factor of 2. This confirms earlier diffusion results with zeolite crystallites of a mean diameter of 3 μm in Kärger, (1971), where essentially the same diffusivities as for the 35 μm sample were observed, when the measuring temperature was low enough (<270 K) to permit the measurement of intracrystalline diffusion. Therefore it should be justified to compare the TFR measurements on 100 μm crystallites with the PFG NMR measurements with any other of the considered zeolites of type NaX if a possible difference of the absolute values by a factor of two is taken into consideration. For this purpose, we have chosen the PFG NMR water diffusivity data for the 35 μm sample after activation mode 3.

TFR Results

The volume, pressure and temperature data are treated in order to obtain either the characteristic functions θ^v_{in} and θ^v_{out} obtained taken the volume as reference, or the characteristic functions θ^p_{in} and θ^p_{out} obtained taken the pressure as reference. As an example, Fig. 8 shows the characteristic functions θ^v_{in} and θ^v_{out} (cf. Eq. (7)) determined from the TFR measurements with Sample I at a temperature of 288 K. It turned out that it was not possible to fit the experimentally determined characteristic functions by model calculations involving

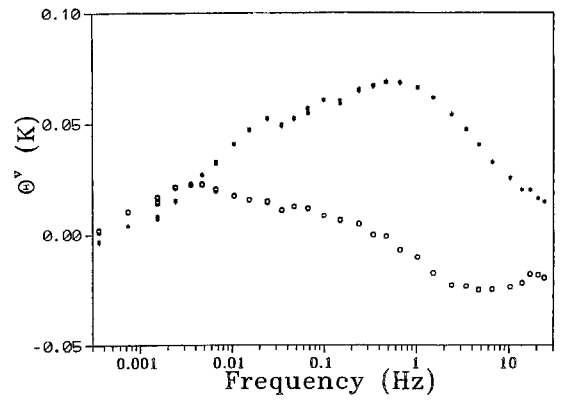

Figure 8. Experimental complex temperature characteristic function: (* * *) in-phase (real part) θ^v_{in} and (o o o) out-of-phase (imaginary part) θ^v_{out} for the Experiment No. 1 (volume taken as reference).

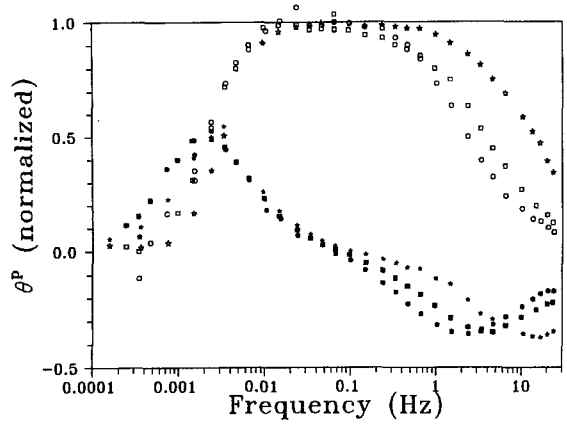

Figure 9. Normalized experimental characteristic functions: θ_{in}^{p} (empty symbol) and θ_{out}^{p} (full symbol): (o o o) Experiment No. 1. (□ □ □) Experiment No. 2. (* * *) Experiment No. 3. The thermal relaxation kinetic domain (maximum of the out-of-phase function) is well separated from the mass transfer kinetic domain (minimum of the out-of-phase function).

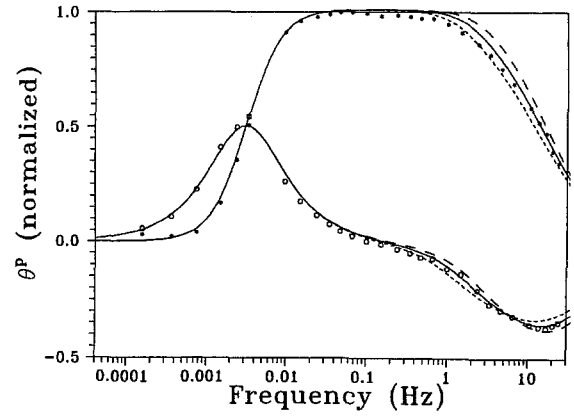

Figure 10. Curve fitting of the Experiment No. 3. Experiment varying D_T alone: (* * *) in-phase. (o o o) out-of-phase. Model: $k = 7.5\ 10^{-4}$ ms^{-1}. (— —) $D_T = 4.5\ 10^{-9}$ m^{2}s^{-1}. (——) $D_T = 3.0\ 10^{-9}$ m^{2}s^{-1}. (____) $D_T = 2.0\ 10^{-9}$ m^{2}s^{-1}.

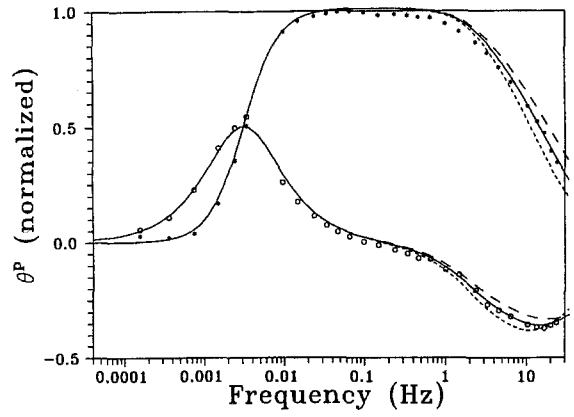

Figure 11. Curve fitting of the Experiment No. 3. Experiment varying k alone: (* * *) in-phase. (o o o) out-of-phase. Model: $D_T = 3.0\ 10^{-9}$ m^{2}s^{-1}. (— —) $k = 1.2\ 10^{-3}$ ms^{-1}. (——) $k = 7.5\ 10^{-4}$ ms^{-1}. (____) $k = 5.0\ 10^{-4}$ ms^{-1}.

intracrystalline diffusion, surface barrier permeation and heat dissipation as possible rate determining processes. We have attributed this discrepancy to water adsorption at the chamber walls. This explanation could be confirmed by blank experiments revealing a pressure response even in the absence of the adsorbent. In such a case the temperature response should be expressed as a function of the measured pressure rather than of the volume with the corresponding characteristic functions given by Eq. (8). Figure 9 shows the pressure related (normalized) characteristic functions θ_{in}^{p} and θ_{out}^{p} experimentally determined in the TFR measurements with Sample I at 288 K, 297 K and 328 K. These functions are clearly different from the functions θ_{in}^{v} and θ_{out}^{v} and are well fitted by the model (see below). This means that such a treatment avoids the need for a blank experiment: in fact, the pressure measurement takes the place of the blank experiment.

The shift of the high frequency part of these functions to higher frequencies with increasing temperature reflects the corresponding decrease of the characteristic times of mass transfer. A quantitative determination of the mass transfer coefficients, via the diffusion coefficient D_T and the surface barrier permeability k, is based on a curve fitting procedure. Figures 10 and 11 show the results obtained for the Sample I at 328 K with the parameters given in the figure legend. By varying the fitting parameters D_T (Fig. 10) and k (Fig. 11), one may also deduce information about the parameter range compatible with the measured response. A summary of the relevant parameters of the TFR experiments and of the kinetic parameters identified by a fitting procedure is given in Tables 2 and 3. It may be observed that the results obtained with different sample thicknesses are not significantly different. This important result can be explained as follows: at sufficient frequency, the crystallites situated inside the bed are not affected by the external pressure variation. The temperature response, as measured by infrared detection, is the response of the surface crystallites, which is thus independent of the bed thickness in first approximation.

For comparison with the diffusivities measured under equilibrium (self-diffusivities D), the diffusivities determined under non-equilibrium conditions ("transport" diffusivities D_T) are generally transferred to

Table 2. Main relevant parameters of the TFR experiments.

Experiment	Sample	Mass mg	P_e Pa	T_e K	q_e kgm^{-3}	ΔH Jkg^{-1}	K_p $kgm^{-3}Pa^{-1}$	K_T $kgm^{-3}Pa^{-1}$	K	γ	Darken factor
1	I	23.5	58	288	426	$3.1\ 10^6$	0.64	−3.06	2.0	3.4	0.087
2	I	23.5	103	297	420	$3.1\ 10^6$	0.39	−3.13	1.3	3.5	0.096
3	I	23.5	660	328	403	$3.1\ 10^6$	0.076	−3.22	0.3	3.8	0.124
4	II	73	37	283	425	$3.1\ 10^6$	0.99	−3.14	9.5	3.5	0.087
5	II	73	153	304	415	$3.1\ 10^6$	0.28	−3.23	2.9	3.7	0.104
6	II	73	830	342	364	$3.2\ 10^6$	0.080	−4.06	0.9	5.2	0.184

Table 3. Identified kinetic parameters from the TFR experiments.

Experiment	D_T $10^{-10}\ m^2s^{-1}$	D_0 $10^{-10}\ m^2s^{-1}$	k $10^{-4}\ ms^{-1}$	τ_D s	τ_s s
1	5.0	0.44	1.3	0.11	0.043
2	7.0	0.67	2.6	0.10	0.028
3	30	3.7	7.5	0.043	0.017
4	3.0	0.26	2.0	0.053	0.008
5	6.8	0.72	12	0.064	0.004
6	16	3.0	8.5	0.053	0.011

"corrected" diffusivities D_0 by using the Darken relation (Kärger and Ruthven, 1992):

$$D_0 = \left[\frac{\partial \ln q}{\partial \ln p}\right]_T D_T \tag{15}$$

with q denoting the adsorbate concentration in equilibrium with sorbate pressure p at temperature T. For small and medium concentrations, D_0 may be expected to be close to the self-diffusivity D (Kärger and Ruthven, 1992; Maginn et al., 1993). For loadings close to saturation the "Darken factor" $\partial \ln q/\partial \ln p$ may become substantial. The values of $\partial \ln q/\partial \ln p$ as calculated from the adsorption isotherms for the relevant experimental conditions are included in Table 2.

Comparison of the Results

Figure 12 provides a comparison between the corrected diffusivities determined from the TFR measurements and the PFG NMR self-diffusivities for water in zeolite NaX. It appears from the representation that the diffusivities determined by both techniques are comparable with each other within the margin of experimental errors. One has to conclude, therefore, that for water in NaX in contrast to the results obtained for some

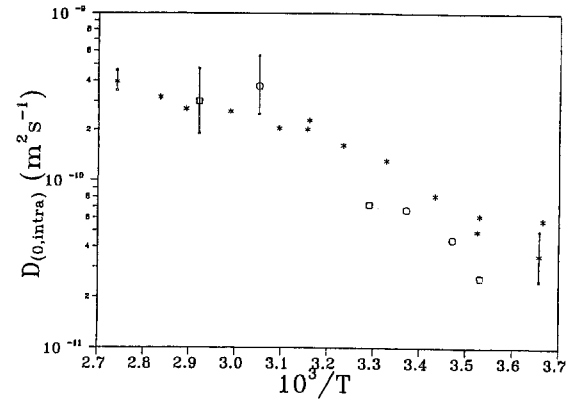

Figure 12. Comparison of the diffusivities ("corrected" diffusivities D_0) of water in NaX obtained by TFR measurements (crystallite diameter 100 μm, activation mode 2 (see Table 1), ~25 molecules per cavity) with PFG NMR diffusivities D_{intra} (crystallite diameter 35 μm, activation mode 3, 26 molecules per cavity—data from (Kärger, 1971)): (o o o) TFR measurements with Sample I. (□□□) TFR measurements with Sample II. (***) PFG.NMR measurements.

n-paraffins in NaX (Ruthven et al., 1991), there is no striking discrepancy in the information about intracrystalline molecular mobility between the equilibrium and non-equilibrium measurements.

The comparison of the temperature dependence of the diffusivities and, thus, of the activation energies, leads to less good agreement. The activation energy as deduced from the PFG NMR data is 19 ± 2 kJ/mole and is 35 ± 11 kJ/mole for the TFR measurements. The uncertainties are the variances of the linear regressions obtained from the experimental data. The value of the activation energy as deduced from PFG-NMR measurements is in good agreement with the activation energy of molecular reorientation in NaX (Pfeifer, 1976) as well as with the activation energy of diffusion in neat water (Weingärtner, 1982). The information about the temperature dependence of the diffusivities from the TFR measurements is less accurate than the results obtained by PFG NMR method since

the temperature interval in the TFR measurements cannot be as large as in PFG NMR measurements and the number of experiments is small. Although the results are not strictly incompatible, it seems that temperature dependence of the diffusivity as given by the TFR method is significantly larger than those given by the PFG-NMR method. Thus it cannot be excluded that the non-equilibrium corrected diffusivity data indicated in Fig. 12 are affected by an inaccuracy in the Darken factors (Eq. 15). It can also not be excluded that the Darken correction gives not an exact correspondence between transport and equilibrium diffusivities, especially at high loadings.

The results given Table 3 show that the best fit of the TFR experimental data is obtained when a small surface barrier is added to the diffusion process. So far it is also not possible to say whether the surface permeability introduced into the mathematical model is anything more than a mere fitting parameter. At present, one could only speculate about the structural and/or microdynamic origin of a surface barrier effect in the sample under study.

Conclusion

The recently introduced thermal frequency response method has been successfully applied to the study of water diffusion in zeolite NaX. It was shown that in this way complications due to water adsorption on the chamber walls may be circumvented. The zeolite samples used in the TFR measurements were not available in an amount large enough to allow PFG NMR self-diffusion measurements. In a complementary PFG NMR study the influence of sample preparation and of the zeolite genesis on the intracrystalline diffusion of water was investigated using NaX samples of smaller crystal size. It was found that for zeolites from different batches, as well as after different modes of sample preparation, the water diffusivities did not differ from each other by more than a factor of about two. Only after a severe hydrothermal pretreatment was a significant change in the diffusion behaviour observed. For moderate sample activation it could be justified, therefore, to compare the diffusivities obtained by PFG NMR and TFR even though it was impossible to use identical zeolite specimens. Within the limits of experimental accuracy, excellent agreement was found between TFR diffusivities determination and PFG-NMR results.

Nomenclature

A_T	Temperature response amplitude	K
A_M	Adiabatic maxima temperature response amplitude	K
C_s	Volumetric heat capacity of the crystals	$J/m^3\ K$
D_T	Transport diffusivity	m^2s^{-1}
D_0	Corrected diffusivity by the Darken law	m^2s^{-1}
D_{intra}	Intracrystalline self diffusivity	m^2s^{-1}
h	Heat transfer coefficient between sample and surroundings	W/m^2K
k	Surface transfer coefficient	ms^{-1}
K	Adsorptive capacity coefficient, dimensionless	
K_p	Derivative of the isotherm with respect to the pressure	kg/m^3Pa
K_T	Derivative of the isotherm with respect to the temperature	kg/m^3K
P	Pressure	Pa
P_e	Mean pressure	Pa
p	Relative pressure response amplitude, dimensionless	
q	Sorbate concentration	kg/m^3
R	Gas constant	J/K
R_c	Crystal radius	m
T	Sample temperature	K
T_e	Temperature of the wall	K
V	Chamber volume	m^3
V_e	Mean chamber volume	m^3
V_s	Sample volume	m^3
v	Relative volume amplitude dimensionless	

Greek Letters

γ	Non-isothermality coefficient	
$\delta_{\text{in}}, \delta_{\text{out}}$	In-phase and out-of-phase pressure response functions	
ΔH	Enthalpy of sorption	J/kg
φ	Phase of the temperature response	rad
ψ	Phase of the pressure response	rad

σ	Shape factor: 0,1 or 2 for sheet, cylinder and sphere respectively	
Θ	Period of the volume modulation	s
$\theta^{v}_{\text{in,out}}$	In-phase and out-of-phase temperature response functions, expressed with respect to the volume	
$\theta^{p}_{\text{in,out}}$	In-phase and out-of-phase temperature response functions, expressed with respect to the pressure	
τ_D	Characteristic time of isothermal diffusion	s
τ_h	Characteristic time of thermal relaxation	s
τ_s	Characteristic time of mass surface transfer	s
ω	Angular frequency	s^{-1}

Acknowledgments

We are obliged to Prof. S. Zhdanov for supplying us with the zeolite samples and to Prof. H. Pfeifer and Prof. R.Q. Snurr for valuable discussions and helpful comments on the manuscript. The Leipzig group acknowledges financial support by the Deutsche Forschungsgemeinschaft (SFB 294) and by the Max-Buchner-Stiftung. The Orsay group acknowledges financial support by the European Community under the Joule program (CEE JOU2-CT 92-0076).

References

Barrer, R.M., *Zeolites and Clay Minerals as Sorbents and Molecular Sieves*, pp. 256–337, Academic Press, London, 1978.

Barrer, R.M. and B.E.F. Fender, "The Diffusion and Sorption of Water in Zeolites-II. Intrinsic and Self-Diffusion," *J. Phys. Chem. Solids*, **21**, 12–24 (1961).

Bourdin, V., Ph. Grenier, F. Meunier, and D.M. Sun, "A Thermal Frequency Response Method for the Determination of Mass Transfer Kinetics in Adsorbents," *AIChE J.*, **42**(3).

Bülow, M. and A. Micke, "Determination of Transport Coefficients in Microporous Solids," *Adsorption*, **1**, 29–48 (1995).

Chen, N.Y., T.F. Degnan, and C.M. Smith, *Molecular Transport and Reaction in Zeolites*, VCH, New York, 1994.

Garcia, S.F. and P.B. Weisz, "Effective Diffusivities in Zeolites," *J. Catal.*, **121**, 294–311 (1990).

Grenier, Ph., F. Meunier, P.G. Gray, J. Kärger, Z. Xu, and D.M. Ruthven, "Diffusion of Methanol in NaX Crystals: Comparison of IR, ZLC and PFG NMR Measurements," *Zeolites*, **14**, 242–249 (1994).

Heink, W., J. Kärger, H. Pfeifer, P. Salverda, K.P. Datema, and A. Nowak, "Self-Diffusion Measurements of *n*-Alkanes in Zeolites NaCaA by Pulsed Field Gradient Nuclear Magnetic Resonance," *J. Chem. Soc. Farad. Trans.*, **88**, 515–519 (1992).

Heink, W., J. Kärger, G. Seiffert, G. Fleischer, and J. Rauchfuß, "PFG NMR Self-Diffusion Measurements with Large Field Gradients," *J. Magn. Reson.*, **A114**, 101–104 (1995).

Kärger, J., "Diffusionuntersuchungen von Wasser an 13X-sowie an 4A-und 5A-Zeolithen mit Hilfe der Methode der gepulsten Feldgradienten," *Z. Phys. Chem., Leipzig*, **248**, 27–41 (1971).

Kärger, J. and D.M. Ruthven, *Diffusion in Zeolites and Other Microporous Solids*, Wiley, New York, 1992.

Maginn, E.J., A.T. Bell, and D.N. Theodorou, "Transport Diffusivity of Methane in Silicalite from Equilibrium and Nonequilibrium Simulations," *J. Phys. Chem.*, **97**, 4173–4181 (1993).

Pfeifer, H., "Surface Phenomena Investigated by Nuclear Magnetic Resonance," *Physics Reports*, **26**, 293–338 (1976).

Pfeifer, H., A. Gutsze, and S.P. Zhdanov, "An Intermediate State of Anomalous High Mobility of Water Molecules Adsorbed in Small Pores of Faujasite Type Zeolites," *J. Coll. Interf. Sci.*, **64**, 412–417 (1978).

Rees, L.V.C., "Exciting New Advances in Diffusion of Sorbates in Zeolites and Microporous Materials," in *Zeolites and Related Microporous Materials: State of the Art 1994*, J. Weitkamp, H.G. Karge, H. Pfeifer, and W. Hölderich (Eds.), pp. 1133–1150, Elsevier, Amsterdam, 1994.

Rios, J.,"Contribution a l'étude d'un Cycle de Pompe à Chaleur à Adsorption à Double Effet Utilisant le Couple Zéolithe 13X-eau," *Thèse*, Paris, 1984.

Ruthven, D.M., *Principles of Adsorption and Adsorption Processes*, pp. 124–173, Wiley, New York, 1984.

Ruthven, D.M., "Diffusion of Xe and CO^2 in 5A Zeolite Crystals," *Zeolites*, **13**, 594 (1993).

Ruthven, D.M., M. Eic, and Z. Xu, "Diffusion of Hydrocarbons in A and X Zeolites and Silicalite" in *Catalysis and Adsorption by Zeolites*, G. Öhlmann, H. Pfeifer, and R. Fricke (Eds.), pp. 233–246, Elsevier, Amsterdam, 1991.

Sahnoune, H. and Ph. Grenier, "Mesure de la Conductivité Thermique d'une Zéolithe," *Chem. Eng. J.*, **40**, 45–54 (1989).

Sun, L.M., F. Meunier, and J. Kärger, "On the Heat Effect in Measurements of Sorption Kinetics by the Frequency Response Method," *Chem. Eng. Sci.*, **48**(4), 725–722, (1993).

Tiselius, A., "Die Diffusion von Wasser in einem Zeolithkristall," *Z. Phys. Chem.*, **169**, 425–458 (1934).

Van den Begin, N.G. and L.V.C. Rees, "Diffusion of Hydrocarbons in Silicalite Using a Frequency Response Method" in *Zeolites: Facts, Figures, Future*, P.A. Jacobs and R.A. van Santen (Eds.), pp. 915–924, Elsevier, Amsterdam, 1989.

Weingärtner, H., "Self-Diffusion in Liquid Water. A Reassessment," *Z. Phys. Chem. Neue Folge*, **132**, 129–149 (1982).

Weisz, P.B., "Diffusion Transport in Chemical Systems-Key Phenomena and Criteria," *Ber. Bunsenges. Phys. Chem.*, **79**, 798–806 (1975).

Yasuda, Y., "Frequency Response Method for Investigation of Gas-Surface Dynamic Phenomena," *Hetero. Chem. Rev.*, **1**, 103–124 (1994).

Zhdanov, S.P., S.S. Chvostchov, and N.N. Samulevitch, *Synthetic Zeolites* (in Russian), pp. 61–64, Khimia, Moscow, 1981.